



Contents lists available at ScienceDirect

Microelectronics Reliability

journal homepage: www.elsevier.com/locate/mr

Magnetic field and current density imaging using off-line lock-in analysis

M. Kögel*, F. Altmann, S. Tismer, S. Brand

Fraunhofer Institute for Microstructure of Materials and Systems IMWS, Halle, Germany

ARTICLE INFO

Article history:

Received 4 July 2016

Accepted 8 July 2016

Available online xxx

Keywords:

Magnetic current imaging

Magnetoresistive sensors

Current density distribution

Magnetic current microscopy

MCI

Lock-in analysis

ABSTRACT

In the current paper the application of a custom developed 2-dimensional scanning magnetic field microscope based on tunnel-magnetoresistive sensors and subsequent qualitative and quantitative analysis is described. To improve sensitivity and to enable the detection and evaluation of phase deviations, an off-line lock-in approach was employed by driving the samples under test with an injected current at a fixed signal frequency. Amplitude and phase evaluation was based on simultaneous acquisition of the reference and the measurement signal obtained from the magnetic field sensor. This off-line lock-in approach enables not just the detection but also the estimation of changes in signal phase caused by capacitive, inductive or ohmic coupling of the induced currents. Furthermore assessed magnetic fields were converted into the current density by solving the inverse magnetic problem and post processing of the acquired signals. For verification of the developed set-up the current density distribution was computed from experimentally acquired magnetic fields for a two-wire test structure. In addition quantitative values of the current density were derived for a calibration pattern containing defined structures. Finally, to evaluate the practical relevance a power MOSFET with unknown defect was analysed and an area of unexpectedly increased magnetic field intensity was observed.

© 2016 Published by Elsevier Ltd.

1. Introduction

Trends in microelectronics continuously push towards increased device performance and functionality by miniaturization and progressive integration. Along with this trend increasing integration rates result in higher structural complexity, thus challenging established failure analysis approaches. Non-destructive inspection methods are commonly pursued for defect localization prior to high resolution physical analyses requiring destructive preparation for the identification of root causes. Magnetic Current Imaging (MCI) enables non-destructive detection of current paths in packaged devices giving access to short circuits, leakage currents, narrow current paths and capacitive coupling [1]. Several methods using commercial equipment employing Superconducting Quantum Interference Devices (SQUIDs) or Giant Magneto Resistive (GMR) sensors have been evaluated for application in failure analysis [1,2]. Another class of commercial devices use sensors based on the tunnel-magnetoresistive effect (TMR) as described in [3]. In general, the relevant quality of such sensor probe is the minimum detectable current and the magnetic sensitivity. Both of these values are frequency dependent, and the former also depends on the spacing between current path

and sensor tip. To maintain superconductivity, SQUIDs need to operate at an ambient temperature close to zero Kelvin, requiring cooling with liquid helium. While these sensors offer major advantages in field- and current sensitivity, the spatial resolution for distances (between probe and sample) below 100 μm is less compared to TMR or GMR sensors (see Table 1). For closer distances the current sensitivity of these sensors show superior performance compared to SQUIDs. Preceding publications showed that sensitivity of TMR sensors improves by a factor of 3–6 at higher frequencies while GMR and SQUID approached their white noise-limited floor at 50 kHz [4]. Consequently, TMR sensors fill the gap between high sensitive SQUIDs and the high spatial resolution of GMR-sensors in the distance range of 1 μm to 100 μm . Besides the much lower price of these probes it is the smaller physical dimensions of TMR sensors that are highly beneficial in practical applications.

The current study describes the development and application of a low-cost custom-built scanning setup for magnetic field and current density imaging based on TMR-sensors. In the present work the current density was computed from experimentally obtained magnetic fields providing access to the current flow with a lateral resolution down to 20 μm . A selection of samples has been investigated to evaluate the potential of this technique for several applications in the field of failure analysis. The first sample was deployed for concept validation while another one with high resistive metal meander lines was measured and

* Corresponding author.

E-mail address: Michael.Kogel@imws.fraunhofer.de (M. Kögel).

Table 1
Comparison of common key parameters for three types of sensors taken from [4].

Specification	GMR	TMR	SQUID
Footprint	1.25 mm ²	0.045 mm ²	3.14 mm ²
Magnetic field sensitivity (10 kHz)	560 nT/Hz ^{1/2}	4.2 nT/Hz ^{1/2}	0.035 nT/Hz ^{1/2}
Current sensitivity ^a (10 kHz)	3.6 μA/Hz ^{1/2}	0.09 μA/Hz ^{1/2}	0.009 μA/Hz ^{1/2}
Current sensitivity ^a (50 kHz)	2.6 μA/Hz ^{1/2}	0.02 μA/Hz ^{1/2}	0.009 μA/Hz ^{1/2}
Intrinsic spatial resolution ^a	0.3 μm	3.8 μm	53 μm

^a Values assumed by a sample distance of 1 μm.

compared to results obtained from Lock-in IR-Thermography (LIT) [5]. Finally, a case study addressing a shorted power MOSFET device was conducted to evaluate applicability of MCI using TMR sensors.

2. Materials and methods

2.1. Sample description

Magnetic field and current imaging was evaluated at three different samples. The experimental setup developed was tested using a PCB structure containing two Cu-lines of width 400 μm and pitch of 1600 μm as shown in Fig. 4. This structure allowed verification of the analysis algorithms for computing the current density distribution from the experimentally assessed magnetic fields.

The second sample shown in Fig. 1 included aluminum metal meander lines with 2 μm linewidth connected by approx. 20 μm lines to bondpads. This structure was used to assess the quantitative magnetic field and gives access to the two-dimensional qualitative current density distribution of the injected current.

In addition to these simplified structures a power MOSFET (see Fig. 2) was investigated for assessing the two-dimensional current density distribution in the metallization pads. This device was electrically failed and a current flow was observed without applying an electric field to the gate.

2.2. Magnetic field imaging

Two-dimensional magnetic field imaging was performed using a custom experimental set-up developed by Fraunhofer IMWS (Halle, Germany). The system consisted of the magnetoresistive sensor probe, a preamplification and filter unit, a motorized xyz-scanner unit, a PC with an integrated analog-digital converter (ADC) interfaced via

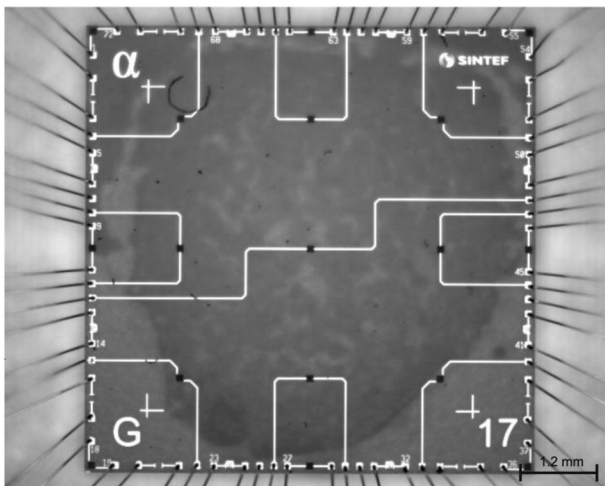


Fig. 1. Thermal image of emissivity (topography) of meander-line sample with dimension of 7 mm × 7 mm – bonded silicon die in chip carrier includes circuit paths on surface (linewidth ~20 μm). Black areas contain meander lines with 2 μm linewidth and increased electrical resistance.

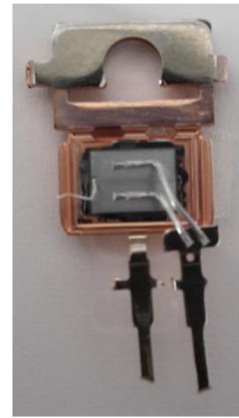


Fig. 2. Power N-Channel 40 V-MOSFET used for inspection of magnetic field and current imaging.

MATLAB and a pair of Helmholtz coils U8481500 (3B Scientific, Hamburg, Germany) for sensor calibration.

For probe-positioning a commercial 3-axis motorized scanner (ITK, Lahnau, Germany) was controlled by a custom software for synchronous motion driving. The magnetoresistive sensor probe was mounted on the z-stage of the scanning unit with the field sensitive direction in the z-orientation. This allows a precise positioning of ~10 μm between the sample surface and the sensor tip. Scanning was performed in a non-contact mode. To avoid any physical influence the sensor was mounted on a flexible assembly which detects the contact forces with a sensitivity of ~20 μN that immediately stops the motion of the scanner unit in contact case. For height calibration the probe tip is manually positioned using a CMOS camera with integrated light source.

The set-up can be operated with two different commercially available TMR probes STJ-220 and STJ-020 (MicroMagnetics, Fall River, Massachusetts, USA). Both types have a linear response over an extended field range (± 0.6 mT) but differ in noise rate and achievable resolution (Table 2) that enable to application tasks depending on the required field sensitivity and sample-probe distance.

The used sensor is interconnected to an Anderson-loop [6] that converts small resistive changes induced by gradients of the magnetic field to a voltage signal. The output signal of the Anderson-loop was amplified by a preamplifier circuit AL-05 (MicroMagnetics) with a gain of 2000 and a bandwidth from DC to 700 kHz. Both parts of the signal reception are calibrated to provide an absolute output of approximate $\sim 20 \text{ VmT}^{-1}$.

To increase the Signal-to-Noise-Ratio (SNR) of the sensor signal it is necessary to reduce the influence of Johnson noise that follows a relationship on f^{-1} . Therefore an alternating current with a fixed frequency between 5 kHz and 40 kHz was injected in the devices under test (DUT). The sinusoidal excitation signal was generated using a 3314 A signal generator (Hewlett-Packard, Palo Alto, California, USA) and amplified using a custom built power amplifier. For enabling lock-in analysis the non-amplified excitation signal was acquired as reference by the NI-9201 ADC (National Instruments, Austin, Texas, USA) at a sampling rate of 120 kHz. While the TMR probe was scanned line-wise across the sample, the amplified sinusoidal current injected into the sample

Table 2
Specifications^a of used TMR-sensors.

Specification	STJ220	STJ020
Footprint	0.56 mm ²	8 μm ²
Magnetic field sensitivity	$\sim 0.5\text{--}15 \text{ mT}^{-1}$	$\sim 7\text{--}20 \text{ mT}^{-1}$
Equivalent field noise (100 Hz)	2 nT/Hz ^{1/2}	50 nT/Hz ^{1/2}
Equivalent field noise (10 kHz)	200 pT/Hz ^{1/2}	5 nT/Hz ^{1/2}

^a Taken from data sheet: <http://www.micromagnetics.com/docs/>.

Download English Version:

<https://daneshyari.com/en/article/4971862>

Download Persian Version:

<https://daneshyari.com/article/4971862>

[Daneshyari.com](https://daneshyari.com)